U.S. ARMY RDECOM

TECHNICAL REPORT RDMR-WS-12-02

OPERATION OF SILICON-ON-INSULATOR (SOI) MICRO-ELECTROMECHANICAL SYSTEMS (MEMS) GYROSCOPIC SENSOR AS A TWO-AXIS ACCELEROMETER

Tracy D. Hudson
Weapons Sciences Directorate
Aviation and Missile Research, Development, and Engineering Center

And

Michael S. Kranz
ENGeniusMicro, LLC
107 Jefferson Street
Huntsville, AL 35801

April 2012

AMRDEC

DESTRUCTION NOTICE

FOR CLASSIFIED DOCUMENTS, FOLLOW THE PROCEDURES IN DoD 5200.22-M, INDUSTRIAL SECURITY MANUAL, SECTION II-19 OR DoD 5200.1-R, INFORMATION SECURITY PROGRAM REGULATION, CHAPTER IX. FOR UNCLASSIFIED, LIMITED DOCUMENTS, DESTROY BY ANY METHOD THAT WILL PREVENT DISCLOSURE OF CONTENTS OR RECONSTRUCTION OF THE DOCUMENT.

DISCLAIMER

THE FINDINGS IN THIS REPORT ARE NOT TO BE CONSTRUED AS AN OFFICIAL DEPARTMENT OF THE ARMY POSITION UNLESS SO DESIGNATED BY OTHER AUTHORIZED DOCUMENTS.

TRADE NAMES

USE OF TRADE NAMES OR MANUFACTURERS IN THIS REPORT DOES NOT CONSTITUTE AN OFFICIAL ENDORSEMENT OR APPROVAL OF THE USE OF SUCH COMMERCIAL HARDWARE OR SOFTWARE.

REPORT DOCUMENTATION PAGE

Form Approved
OMB No. 074-0188

1. AGENCY USE ONLY	2. REPORT DATE	3. REPORT TYPE AND DATES COVERED
	April 2012	Final

4. TITLE AND SUBTITLE
Operation of Silicon-on-Insulator (SOI) Micro-ElectroMechanical Systems (MEMS) Gyroscopic Sensor as a Two-Axis Accelerometer

5. FUNDING NUMBERS

6. **AUTHOR**(S)
Tracy D. Hudson and Michael S. Kranz

7. PERFORMING ORGANIZATION NAME(S) AND ADDRESS(ES)
Commander, U.S. Army Research, Development, and Engineering Command
ATTN: RDMR-WSI
Redstone Arsenal, AL 35898-5000

8. PERFORMING ORGANIZATION REPORT NUMBER
TR-RDMR-WS-12-02

9. SPONSORING / MONITORING AGENCY NAME(S) AND ADDRESS(ES)

10. SPONSORING / MONITORING AGENCY REPORT NUMBER

11. SUPPLEMENTARY NOTES

12a. DISTRIBUTION / AVAILABILITY STATEMENT
Approved for public release; distribution is unlimited.

12b. DISTRIBUTION CODE
A

13. ABSTRACT ***(Maximum 200 Words)***

This report documents the idea or concept of operating an existing Silicon-on-Insulator (SOI) Micro-ElectroMechanical Systems (MEMS) gyroscopic sensor previously developed in the early-2000s under MEMS-Based Angular Rate Sensor (MBARS) and MicroControlled Array Sensors (mCAS). This report serves as documented evidence for future use of this open-sourced idea of the measurement of two-axis of linear acceleration from a previous sensor originally designed to operate as a single-axis rotation sensor.

14. SUBJECT TERMS
Silicon-on-Insulator (SOI) sensors, inertial technology, Micro-ElectroMechanical Systems (MEMS), gyroscope, accelerometers.

15. NUMBER OF PAGES
22

16. PRICE CODE

17. SECURITY CLASSIFICATION OF REPORT	18. SECURITY CLASSIFICATION OF THIS PAGE	19. SECURITY CLASSIFICATION OF ABSTRACT	20. LIMITATION OF ABSTRACT
UNCLASSIFIED	UNCLASSIFIED	UNCLASSIFIED	SAR

NSN 7540-**01**-280-5500

Standard Form 298 (Rev. 2-89)
Prescribed by ANSI Std. Z39-18
298-102

TABLE OF CONTENTS

LIST OF ILLUSTRATIONS

I. INTRODUCTION

This report documents the idea or concept of operating an existing Silicon-on-Insulator (SOI) Micro-ElectroMechanical Systems (MEMS) gyroscopic sensor previously developed in the early-2000s under MEMS-based Angular Rate Sensor (MBARS) and MicroControlled Array Sensors (mCAS) [1,2,3]. This report serves as documented evidence for future use of this open-sourced idea of the measurement of two-axis of linear acceleration from a previous sensor originally designed to operate as a single-axis rotation sensor.

II. GYROSCOPE CHIP AS A TWO-AXIS ACCELEROMETER

This section presents the development of the equations that enable the gyro system to function as a two-axis (X-axis and Y-axis) accelerometer while functioning as a Z-axis rate gyro. When the mass of the gyro is subjected to a force due to vibration, the mass is displaced in the direction of the force. This displacement is in addition to and independent of any gyro oscillations involved in rotation rate measurements, but motions due to vibrations can affect the gyro's oscillation pattern. If the frequency of the vibration is much less (a factor of 10 or more) than the resonant frequency, these displacements can be accurately detected by the gyro's electronics/software. As the vibration frequency approaches the excitation frequency (ω), the resultant motion appears to be at the beat frequency between the vibration frequency and ω. The physical effect detected depends on the axis (excitation or sense) in which the displacement occurs.

If the displacement is in the direction of the sense axis, then the vibrations can be detected as the average displacement of the mass for each ω period. The sense circuit is designed to measure the amplitude of any oscillation produced by the rotation-induced Coriolis force at ω. The electronics accomplish this by generating sense signals at 256 times ω (approximately 1 megahertz) and measuring the mass' position 256 times each excitation period. The software can then demodulate this signal using a method described in the appendix, as originally published in a 2004 contract report [4]. An average non-zero mass displacement would manifest itself as the constant non-zero value in the Inphase and Quadrature (IQ) demodulation of the sense signal. That is, to measure the displacement due to vibration, sum all the partial signal sums computed in the IQ ω demodulation. This calculation is basically a by-product of the sense demodulation that is already being computed and adds little extra computation time.

If the displacement is in the direction of the excitation axis, then the vibrations can be detected as the average difference between the two excitation diametrically opposite capacitors. Any mismatch between these capacitors produces a signal at ω, as opposed to the excitation amplitude signal produced at 2 ω. Other signal mismatches (that is, mismatch between bias voltages and excitation voltage amplitudes) also produce signals at ω; however, these are constant with time but do vary with temperature. Therefore, to detect a vibration in the excitation axis direction, the software needs to demodulate the excitation signal at ω. The software is already demodulating the signal at 2 ω to track the resonant frequency. To demodulate the excitation signal at ω, partial signal sums need to be summed in a different order, as explained in the appendix. This requires very little additional computation time.

Thus, both the X-axis and Y-axis accelerations can be measured at the same time while the chip is functioning as a gyro with very little additional processor computational time and no additional electronic circuitry.

III. SENSE AXIS SATURATION AND HIGH ROTATION RATE MEASUREMENTS

This section presents the development of the equations that describe the sense axis saturation phenomenon and the excitation axis amplitude attenuation phenomenon. These equations also suggest a method to measure the MEMS gyro rotation rate even after the sense channel output has saturated. In testing gyros, it has been noted that as the rotation rate increases (1,000 to 2,000 degrees per second), the sense channel output increases in a non-linear manner and usually saturates somewhere between 1,500 and 2,000 degrees per second. In the past, this effect has been attributed to the electronics saturating and spring softening, but this section develops equations that explain the phenomenon and suggest that the saturation is due to cross-coupled Coriolis forces in the gyro. The equations suggest a way to measure the rotation rate beyond the rate at which the sense signal stops increasing. They also suggest methods to linearize the sense and excitation outputs over limited ranges.

In essence, as the rotation rate increases, the sense signal increases but at an ever-decreasing rate and eventually saturates. Also, the excitation signal decreases but at an ever-increasing rate even past the rotation rate at which the sense signal saturates. The following is a simple example of an algorithm that uses both the sense and excitation signal to calculate rotation rate:

- Determine the break rotation rate (Ω_B), that is, where $\left(2m\Omega_B\omega K_\omega\right)$ =1, for the gyro chip.
- Use this to linearize the sense signal up to a predetermined rotation rate ($\Omega_1 = \Omega_B/2$).
- Use the sense output to compute the rotation rate between 0 and Ω_1.
- Use this to linearize the excitation signal from Ω_1 on. Use the excitation output to compute the rotation rate above Ω_1.

The following subsections develop the equation for cross-coupled Coriolis forces in the MEMS gyro.

A. Background

There are two paradigms in which vibration gyroscopes operate—the constant excitation amplitude and excitation force paradigms. Both paradigms assume that a mechanical mass/spring system, free to oscillate along two-axis (an excitation axis (X-axis) and a sense axis (Y-axis)), is subject to a rotation around the third axis (Z-axis). A periodic electrostatic force is applied along the excitation axis. Rotation produces an oscillation along the sense axis, the amplitude of which is proportional to the rate of rotation.

Equations 1 and 2 are relevant equations of motion for this system, where *x* is the excitation axis and *y* is the sense axis:

$$\ddot{x} = -\omega_X^2 x - \frac{\omega_X}{Q}\dot{x} - \frac{F_X}{m} + x\Omega^2 + y\dot{\Omega} + 2\Omega\dot{y} - a_X \cos\theta - a_Y \sin\theta \tag{1}$$

and

$$\ddot{y} = -\omega_Y^2 y - \frac{\omega_Y}{Q}\dot{y} - 2\Omega\dot{x} + y\Omega^2 - x\dot{\Omega} + a_X \sin\theta - a_Y \cos\theta . \tag{2}$$

Equations 1 and 2 have units of acceleration (in meters per second squared) but can be converted to force by multiplying by the mass (m) (in kilograms) of the proof mass.

For this discussion, the previous equations will be simplified. This will emphasize the results being derived. If these assumptions are not made, the resultant equations will be almost the same as the ones derived but more algebraically complex. Assume there are no external accelerations, that is, the m is not subject to a gravitational acceleration or external vibrations, then $a_y = a_x = 0$. Also, assume that both axes have the same resonant frequency, that is, $\omega_x = \omega_y = \omega$, the resonant frequency of the mechanical system. Then, these equations can be rewritten as

$$y\dot{\Omega} + 2\Omega\dot{y} - .\frac{F_X}{m} = \ddot{x} + \dot{x}\frac{\omega}{Q} + x\left(\omega^2 - \Omega^2\right) \tag{3}$$

and

$$-2\Omega\dot{x} - x\dot{\Omega} = \ddot{y} + \dot{y}\frac{\omega}{Q} + y\left(\omega^2 - \Omega^2\right). \tag{4}$$

The right-hand side of each equation is the equation of motion for a mass/spring mechanical system. The left-hand side of each equation shows the forcing functions (as accelerations) and the cross coupling between the two-axis.

Further simplify Equations 3 and 4 by assuming that the system is interrogated only at constant rotation, that is, $\dot{\Omega} = 0$. Also, realize that ω is greater than 3,000 hertz, while Ω is approximately 8.3 hertz at a maximum rotation rate of 3,000 degrees per second. Note that (ω^2 - Ω^2) $\approx \omega^2$. Thus, Equations 3 and 4 can be rewritten as

$$2\Omega\dot{y} - .\frac{F_X}{m} = \ddot{x} + \dot{x}\frac{\omega}{Q} + x\omega^2 \tag{5}$$

and

$$-2\Omega\dot{x} = \ddot{y} + \dot{y}\frac{\omega}{Q} + y\omega^2 . \tag{6}$$

Note that there is a set of cross-coupled, second order, linear, differential equations. Assume that F_x is a sinusoid at the resonant frequency, that is, $F_x = F_o \sin(\omega t)$.

Looking at the previous equations, note that when there is no Z-axis rotation (that is, $\Omega = 0$), the equations are not coupled, there is no Coriolis acceleration, and the X-axis oscillation is only caused by the electrostatic forcing function. Depending on initial conditions, the amplitude of the X-axis oscillation asymptotically grows until the forcing function energy is equal to the energy being dissipated by the dissipation constant (heat loss), and then the amplitude remains constant.

A rotation along the Z-axis produces a Coriolis acceleration along the Y-axis (left-hand side of Equation 6) which sets up a sinusoidal oscillation, the amplitude of which can be measured and is proportional to the rotation rate. The Y-axis oscillation in the presence of the Z-axis rotation produces an oscillation along the X-axis, as seen in Equation 5. The X-axis acceleration opposes the electrostatic forcing acceleration. If uncompensated for, the X-axis Coriolis acceleration will reduce the amplitude of the X-axis oscillation.

B. The CEAP

In the Constant Excitation Amplitude Paradigm (CEAP), as the gyro is rotated, the amplitude of the X-axis oscillation is maintained by increasing the electrostatic force's amplitude to counteract the X-axis Coriolis acceleration. Thus, the electrostatic forcing function can be divided into two terms:

$$F_X = F_K^x + F_C^x , \tag{7}$$

where, F_K^x is the constant electrostatic force needed to maintain a constant X-axis oscillation, and F_C^x is the electrostatic force needed to just balance the X-axis Coriolis force, that is:

$$F_C^x = 2m\Omega(t)\dot{y}(t) . \tag{8}$$

Since the amplitude of the X-axis oscillation is maintained at a constant level, the Y-axis Coriolis force equation can be written in a straightforward way as

$$F_C = -2m\Omega(t)\dot{x}(t) , \tag{9}$$

where, m is the gyro's mass, $\Omega(t)$ is the Z-axis rotation rate (in radians), and $\dot{x}(t)$ is the velocity of m along the X-axis (see Equation 6). Since the amplitude of $\dot{x}(t)$ is being maintained at a constant value for Coriolis measurements, there is no need to be concerned about the Y-axis oscillations being fed back to the X-axis because it does not have any impact on $\dot{x}(t)$.

Therefore, in CEAP, the amplitude of the excitation oscillation must be measured. This amplitude measurement is used in a closed-loop feedback control system to continuously change the gain of the forcing function amplifier as the rotation rate changes in order to maintain a constant X-axis oscillation amplitude. In an ideal system, the amplitude could be perfectly maintained; however, in the real world, there will always be errors. As the rotation rate increases, the error in excitation amplitude will increase, and depending on the feedback loop coefficients, the feedback loop may have small error oscillation.

C. The CEFP

In the Constant Excitation Force Paradigm (CEFP), the forcing function amplitude is constant irrespective of the gyro's rotation. As seen from Equations 5 and 6, the force (acceleration) equations for the gyro system are a set of cross-coupled, second-order, linear, differential equations. This implies that as the rotation rate changes, the X-axis oscillation amplitude changes. When there is no rotation, the X-axis amplitude is a maximum. As the rotation increases, the X-axis amplitude decreases as the Y-axis oscillation amplitude increases. This can be thought of as an iterative process that tracks the rotation rate.

Thus, Equation 9 cannot be used to accurately determine the rotation rate because the amplitude of $\dot{x}(t)$ is a function of the rotation rate Ω. When the gyro is rotated along the Z-axis, the solution to the two equations can be thought of as a convergent spiral of interactive forces being generated between the Y-axis Coriolis produced force and the X-axis Coriolis produced force. A forcing function produces a given $\dot{x}(t)$ which produces a Y-axis Coriolis force which, in turn, produces a X-axis Coriolis force which changes the net X-axis force, changing $\dot{x}(t)$, which then changes the Y-axis Coriolis force, and so forth.

Since the electrostatic forcing function is a sinusoid, both $\dot{x}(t)$ and $\dot{y}(t)$ will be sinusoids at the same frequency, and only the amplitudes and relative phases of $\dot{x}(t)$ and $\dot{y}(t)$ need to be determined. Defining the X-axis acceleration function as

$$F_E(t) = 2m\Omega\dot{y} - F_X \sin(\omega t) = F_{Eo} \sin(\omega t). \tag{10}$$

It has been shown in Equation 4 that if the X-axis position is defined as

$$x = x_o \sin(\omega t + \phi), \tag{11}$$

then a solution to Equation 5 is when

$$x_o = F_{Eo} K_\omega \quad , \tag{12}$$

where K_ω is the physical system gain. Since ω is at the system resonance frequency, φ ≈ -90 degrees and

$$\dot{x} = x_o \omega \cos(\omega t - 90) = -x_o \omega \sin(\omega t). \tag{13}$$

First, define the Y-axis force as

$$-2m\Omega\dot{x} = 2m\Omega\omega x_o \sin(\omega t), \tag{14}$$

and the Y-axis position as

$$y = y_o \sin(\omega t + \theta). \tag{15}$$

This results in a solution of Equation 6 where,

$$y_o = 2m\Omega\omega K_\omega x_o . \tag{16}$$

Again, since ω is at the system resonance ($\theta \approx -90$ degrees), the results are

$$\dot{y} = y_o \omega \cos(\omega t - 90) = -y_o \omega \sin(\omega t) . \tag{17}$$

Revisiting Equation 5, the results are

$$2m\Omega\dot{y} - F_X \sin(\omega t) = F_{Eo} \sin(\omega t) = -\left(2m\Omega\omega\right)^2 x_o K_\omega \sin(\omega t) - F_X \sin(\omega t) = \frac{x_o \sin(\omega t)}{K_\omega}, \tag{18}$$

which can be rewritten as

$$-F_X = \frac{x_o}{K_\omega} + \left(2m\Omega\omega\right)^2 x_o K_\omega \tag{19}$$

or

$$-F_X K_\omega = x_o \left(1 + \left(2m\Omega\omega K_\omega\right)^2\right) \tag{20}$$

or

$$x_o = \frac{-F_X K_\omega}{\left(1 + \left(2m\Omega\omega K_\omega\right)^2\right)} . \tag{21}$$

And thus, the equation for y_o becomes

$$y_o = \frac{-F_X K_\omega \left(2m\Omega\omega K_\omega\right)}{\left(1 + \left(2m\Omega\omega K_\omega\right)^2\right)} . \tag{22}$$

Figure 1 shows the normalized trend for the two signals x_o and y_o given that $\left(2m\Omega\omega K_\omega\right) = 1$ at $\Omega = 2{,}000$ degrees per second.

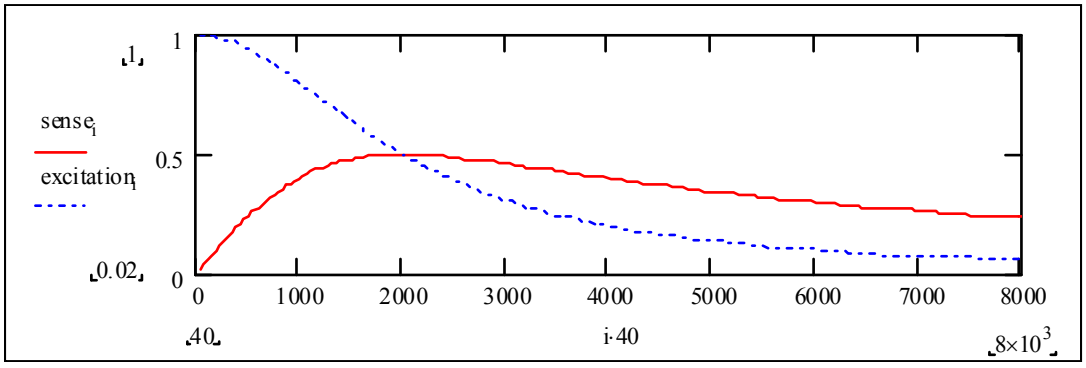

Figure 1. Graph of Normalized Trend for Two Signals

The equation for x_o predicts some interesting results when the gyro is rotated. For the excitation or X-axis:

- The excitation amplitude starts off at its maximum and decreased as Ω increases.
- The amplitude decreases in a parabolic like fashion until it reaches ½, when $(2m\Omega\omega K_\omega) = 1$. In our gyro system, $(2m\Omega\omega K_\omega) = 1$, theoretically, at approximately Ω = 2,000 degrees per second.
- After $(2m\Omega\omega K_\omega) = 1$, the amplitude starts decreasing more as the square of Ω.

For the sense or Y-axis:

- The sense amplitude starts off at zero, and the rate of increase decreases in a parabolic fashion.
- For small Ω, the change is almost linear.
- After $(2m\Omega\omega K_\omega) = 1$, the Coriolis amplitude decreases more linearly as Ω increases. (The gyro was not spun faster than 2,000 degrees per second to record data due to noise in the communication channel.)

The system implications are:

- Use the Coriolis signal to measure small rotation rates and switch to the excitation signal to measure larger rotation rates.
- Use both to measure rates in a band in between.
- The signal saturation on the sense output is not caused by electronics saturation.

IV. GYRO EXCITATION AND CORIOLIS MEASUREMENTS

The previous reference phenomenon has been observed in gyro output signals. The amplitude of the excitation signal starts decreasing in small steps, and as the rotation rate increases, the size of the steps increase. The sense signal starts increasing linearly and seems to be reaching an asymptote as the rate increases. For example, in the following test consisting of uniform rate step size changes shown in Figure 2, the corresponding sense signal's step size decreases to a point of being difficult to notice, that is, the sense signal output "saturates," as shown by Figure 3. The excitation signal shown in Figure 4 also decreased in distinct step as the rate increases. At first, the decreases are relatively small, but at larger rates, the decreases are larger for the same size rate increase.

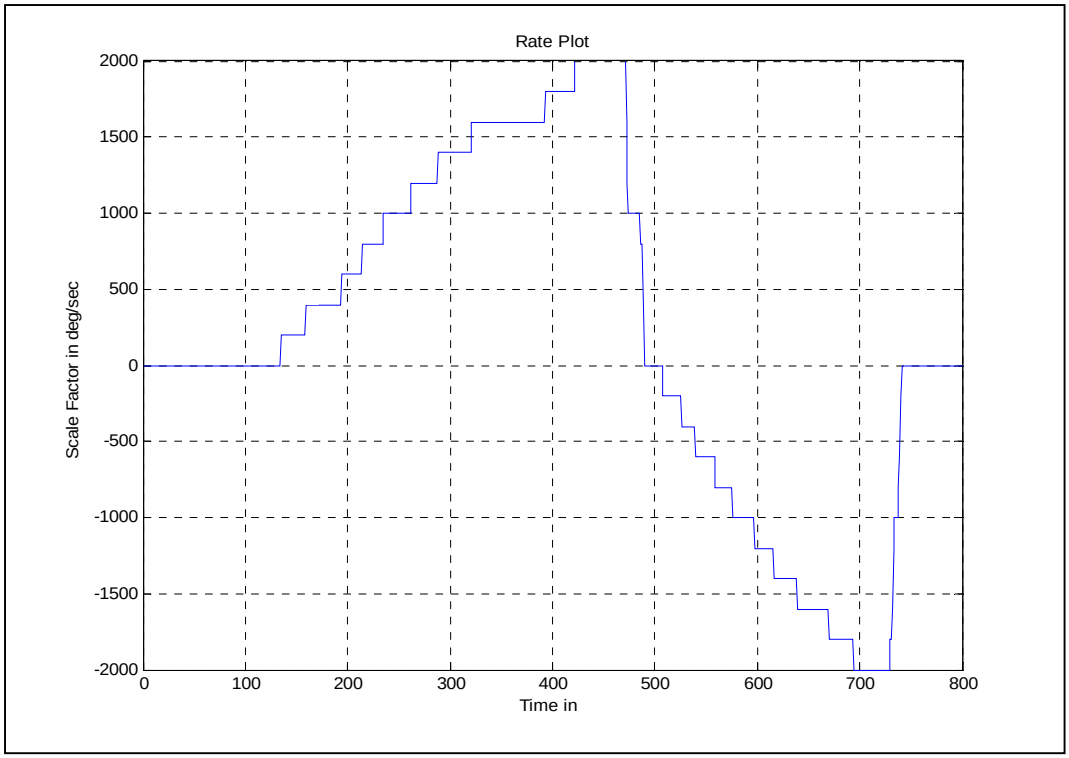

Figure 2. Gyro Rotation Rate in Degrees Per Second

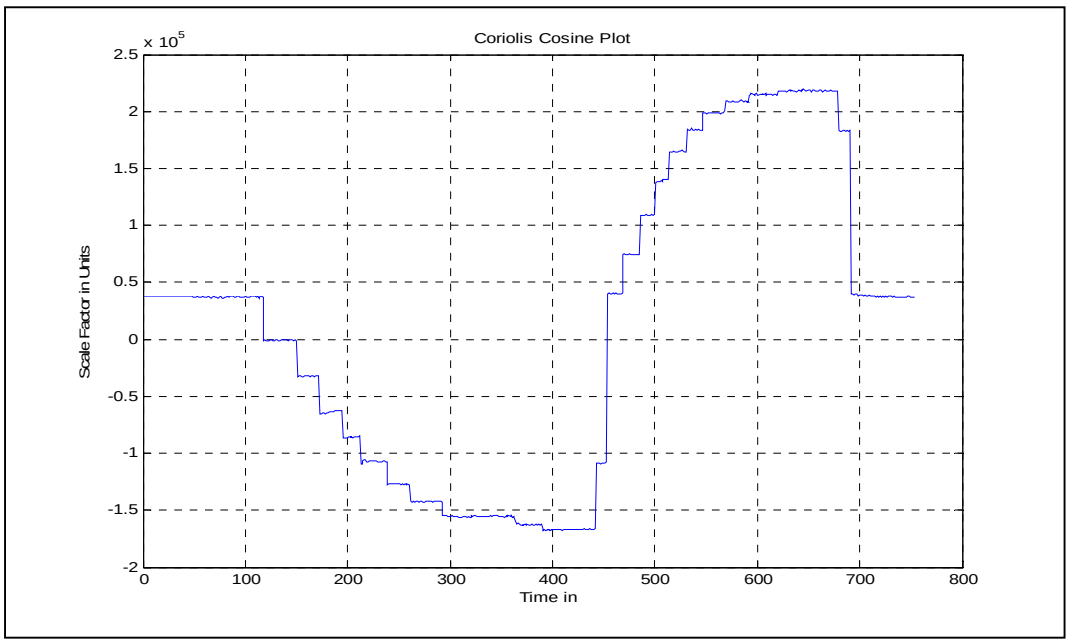

Figure 3. Measured Sense Signal Output

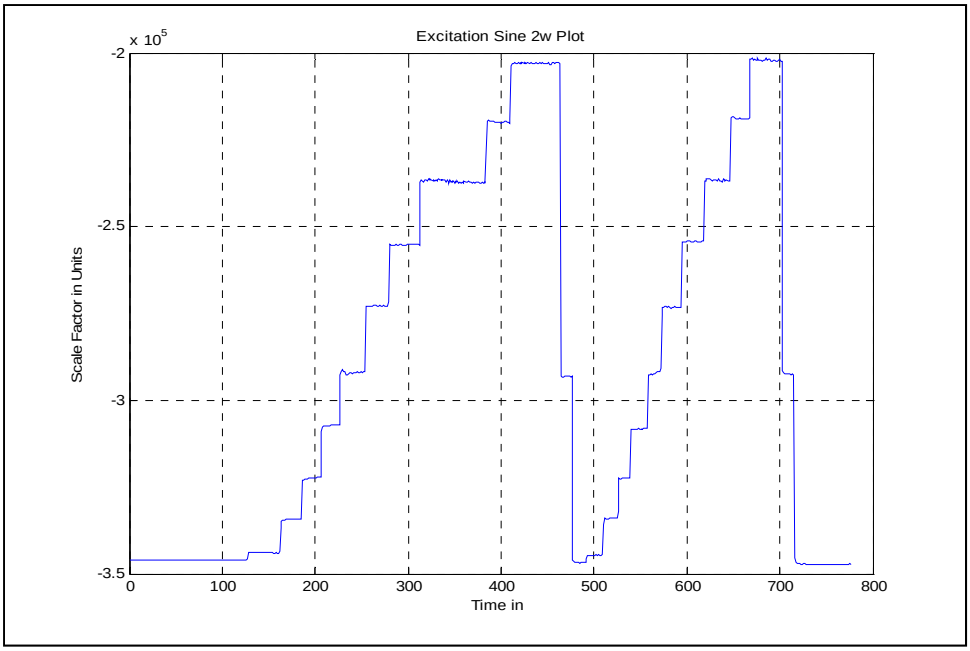

Figure 4. Measured Excitation Signal Amplitude

V. TEST DATA OF GYRO CHIP TO MEASURE ACCELERATION

In later tests on the Serial Number (SN) 854 gyro, the reference accelerometer failed, so there was no way to determine the acceleration being applied to the gyro. Figure 5 shows a portion of an acceleration test. The graph indicates the applied acceleration frequency as a function of time, starting with a 15-hertz signal, progressing to 0 hertz, continuing with a 20-hertz signal, and so forth. Figure 6 shows the corresponding response on the sense axis acceleration channel. The data sampling rate was such that any acceleration frequency greater that approximately 5 hertz would be aliased. Thus, all of the acceleration measurements in this plot are aliased, and no clean sine wave signals can be recorded. When the reference accelerometer worked, it measured low-frequency acceleration at approximately 0.05 *g*. The measurement of the applied acceleration can be seen in the changes in amplitude of the sense axis channel corresponding to the time when the acceleration was applied.

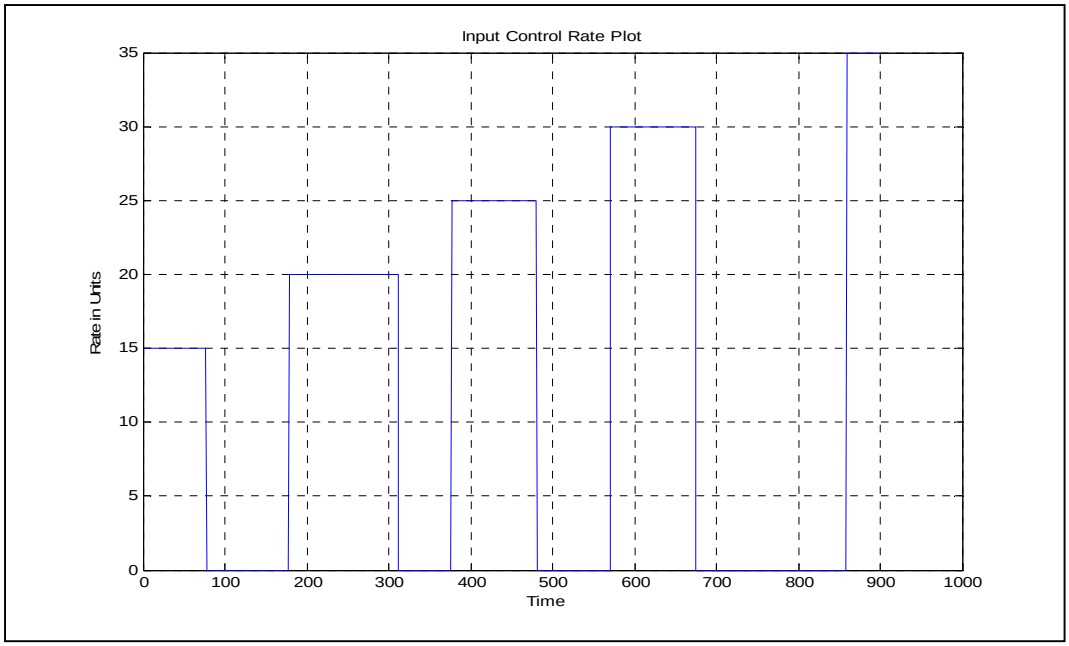

Figure 5. SN854 Gyro Expanded View Showing Applied Acceleration Frequency with Respect to Time

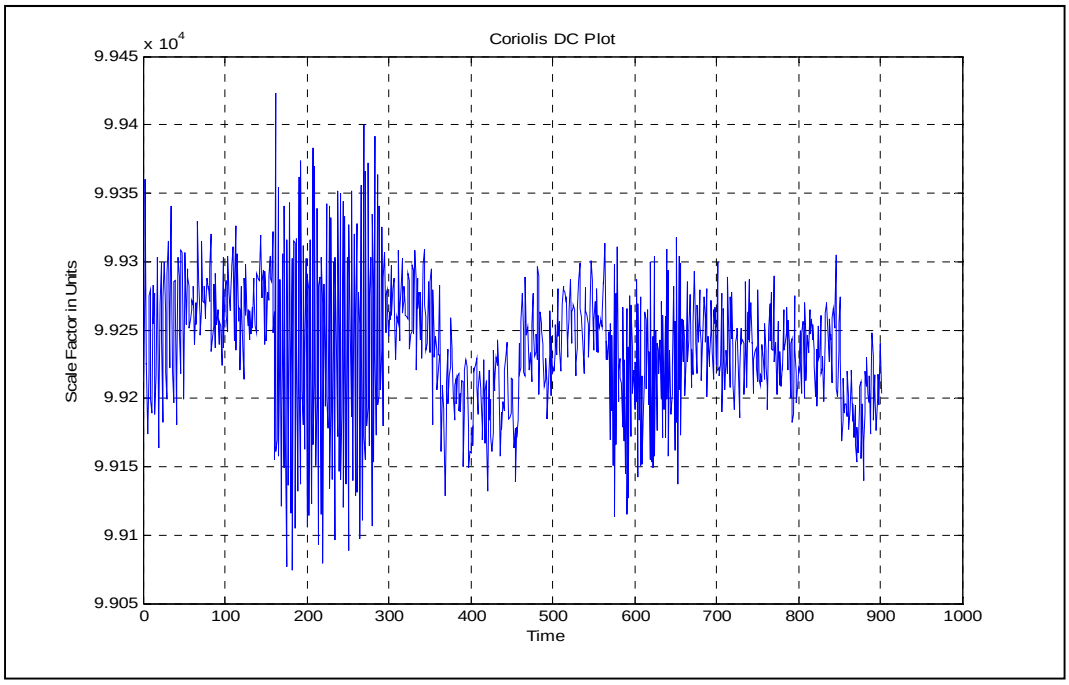

Figure 6. SN854 Gyro Expanded View Showing Acceleration Response on the Sense Acceleration Channel

VI. CONCLUSION

To compensate for the effects of vibration on the gyro required the ability to measure the vibrations. Two methods to measure vibration were pursued: separate accelerometers and the gyro (also acting as accelerometers). The gyro (also acting as accelerometers) proved to be the easiest to implement. Gyro assemblies were vibrated in all three axes, and both excitation and sense signal outputs were recorded. The gyros showed a white noise type of reaction to low-frequency vibration. At frequencies around ω, standing waves were observed. True environmental vibrations would not be at a pure frequency; therefore, these standing waves would not occur. No feasible compensation algorithms were developed.

Equations were developed that predict the changes in both the excitation and sense signal levels as rotation rates increase to higher rates. These effects are practically noticeable at rotation rates greater than 1,000 degrees per second. These equations predict the saturation of the sense output at rotation rates that depend on the physical parameters of the gyro chip. For the current gyro design, the saturation rotation rate was calculated to be approximately 2,000 degrees per second. There has been no testing above 2,000 degrees per second because of the noise on the signal lines through the slip rings on the high-speed rate table located at Aviation and Missile Research, Development, and Engineering Center (AMRDEC). The predicted results were observed in rotation rate tests. These equations also suggest possible algorithms to measure the rotation rate while the sense signal is approaching saturation and possibly up to twice the sense axis saturation rotation rate.

REFERENCES

1. Hudson, T. D.; Burgett, S.; Ruffin, P.; Kranz, M.; McKee, J.; Whitley, M.; Buncick, M.; and Tuck, E., "High Performance Microfabricated Angular Rate Sensor," Journal of Microlithography, Microfabrication, and Microsystems, Volume 4, October through December 2005.

2. Kranz, M. and Holt, S.B, "SOI MEMS Gyroscope Having Three-Fold Symmetry," U.S. Patent Number 7, 267,005, 11 September 2007.

3. Hudson, Tracy D., "Statistical Characterization of an Array of MEMS Based Gyroscopic Inertial Sensors," TR-RDMR-WS-11-03, U.S. Army Aviation and Missile Research, Development, and Engineering Center (AMRDEC), Redstone Arsenal, AL, February 2011.

4. Reiner, Philip, "MEMS, Fiber, and Nanotechnology Support: MBARS Electronics Miniaturization for CKEM Flight Test and MBARS Technology," CDRL 0002-Final Technical Report, DAAH01-00-D-0016/0019, Morgan Research Corporation, Huntsville, AL, June through December 2004.

LIST OF ACRONYMS AND ABBREVIATIONS

AMRDEC	Aviation and Missile Research, Development, and Engineering Center
CEAP	Constant Excitation Amplitude Paradigm
CEFP	Constant Excitation Force Paradigm
g	Gravity
IQ	Inphase and Quadrature
MBARS	MEMS-Based Angular Rate Sensors
mCAS	MicroControlled Array Sensors
MEMS	Micro-ElectroMechanical Systems
SN	Serial Number
SOI	Silicon-on-Insulator
ω	Excitation Frequency

APPENDIX
DERIVATION OF THE EQUATIONS FOR THE IQ DEMODULATION METHOD

Derivation of the Equations for the In-phase / Quadrature Demodulation Method

This Appendix presents the demodulation method used to determine the excitation signal amplitude (at 2ω), the excitation axis acceleration (at ω), and the sense signal amplitude (at ω). The method used is referred to as In phase / Quadrature (IQ) demodulation. It is easy to perform in the digital domain. Starting with the theory, in IQ demodulation at ω, the signal is multiplied by both sin(ωt) and cos(ωt), summed over an integral number of periods, squared, and added together, and then the square root is taken. The following equations illustrate this process, where N is any positive integer and T is the period of ω.

$$IQ..1)...Q = \frac{1}{NT}\int_0^{NT} A\sin(\omega t+\phi)\cos\omega t = \frac{A}{2NT}\int_0^{NT}\sin\phi + \sin(2\omega t+\phi) = \frac{A}{2}\sin\phi\,,$$

$$IQ..2)...I = \frac{1}{NT}\int_0^{NT} A\sin(\omega t+\phi)\sin\omega t = \frac{A}{2NT}\int_0^{NT}\cos(\phi) - \cos(2\omega t+\phi) = \frac{A}{2}\cos\phi\,, \quad \textit{and}$$

$$IQ..3)...I^2+Q^2 = \left(\frac{A}{2}\sin\phi\right)^2 + \left(\frac{A}{2}\cos\phi\right)^2 = \frac{A^2}{4}\left(\sin^2\phi+\cos^2\phi\right) = \frac{A^2}{4}.$$

Along the same line of reasoning, the equation for i_z (from equation 33 of the Excitation Appendix) can be written as

$$IQ..4)...\left(\frac{1}{NT}\int_0^{NT} i_z\sin 2\omega t\right)^2 + \left(\frac{1}{NT}\int_0^{NT} i_z\cos 2\omega t\right)^2 = (x_o KV\omega)^2\,, \quad \textit{and}$$

$$IQ..5)...\frac{\sin\phi}{\cos\phi} = \tan\phi = \frac{\frac{1}{NT}\int_0^{NT} i_z\cos 2\omega}{\frac{1}{NT}\int_0^{NT} i_z\sin 2\omega t}.$$

Now define XIQ as

$$IQ..6)...XIQ^2 = \left(\frac{1}{NT}\int_0^{NT} i_z\sin 2\omega t\right)^2 + \left(\frac{1}{NT}\int_0^{NT} i_z\cos 2\omega t\right)^2, \textit{then}$$

$$IQ..7)..x_o = \frac{XIQ}{KV\omega}.$$

Now let us assume that we are computing IQ using a computer. Then the first simplification is to multiply the signal by a unity amplitude square wave at ω and 2ω. The sine wave would be replaced with a square wave that goes positive at time 0. The cosine wave would be replace with a square wave that is delayed by 90° or ¼ cycle. Then we notice that we do not have to multiply the signal by the square wave amplitude. We only have to sum the signal

samples in each time interval when the square wave is a constant. Then we would subtract the integral sum when the square wave amplitude was -1 from the integral sum when the square wave amplitude was +1. Now we notice that to demodulate at ω, if we divide the signal period into 4 equal time intervals (T1, T2, T3, and T4) and form four sums, i.e., the sum of all the signal measurements in each time interval, we can calculate I and Q with the same data. That is: $I = T1 + T2 - T3 - T4$, and $Q = -T1 + T2 + T3 - T4$. We now notice that if we divide the signal period into eight equal time intervals and combine, i.e., add or subtract, the measurements in the correct order, we can demodulate signals at both ω and 2ω at the same time using the same signal sums. This is the method used to demodulate the excitation signal (at ω and 2ω) and the sense signal (at ω). To calculate the DC value or average of a signal we only need to sum the signal in all of the time intervals.

INITIAL DISTRIBUTION LIST

		Copies
Weapon Systems Technology Information Analysis Center Alion Science and Technology 201 Mill Street Rome, NY 13440	Ms. Gina Nash gnash@alionscience.com	Electronic
Defense Technical Information Center 8725 John J. Kingman Rd., Suite 0944 Fort Belvoir, VA 22060-6218	Mr. Jack L. Rike jrike@dtic.mil	Electronic
AMSAM-L	Ms. Anne C. Lanteigne anne.lanteigne@us.army.mil	Electronic
	Mr. Michael K. Gray michael.k.gray@us.army.mil	Electronic
RDMR		Electronic
RDMR-CSI		Electronic
RDMR	C. Stephen Cornelius Steve.Cornelius@us.army.mil	Electronic
RDMR-ASP	Mr. Ron Schmalbach Ron.Schmalbach@us.army.mil	Electronic
RDMR-WSI	Wayne Davenport Wayne.Davenport@us.army.mil	Electronic
	Dr. Tracy D. Hudson Tracy.Hudson@us.army.mil	Electronic/Hardcopy
RDMR-WDR	Dr. Paul Ruffin Paul.Ruffin@us.army.mil	Electronic
RDMR-WDG-N	Brian Grantham Brian.E.Grantham@us.army.mil	Electronic
	Clinton Blankenship Clint.Blankenship1@us.army.mil	Electronic
ENGenius Micro, LLC 107 Jefferson Street Huntsville, AL 35801	Michael Kranz Michael.Kranz@engeniusmicro.com	Electronic